

High-accuracy models for iris recognition with merging features



Hind Moutaz Al-Dabbas^{1,*}, Raghad Abdulaali Azeez², Akbas Ezaldeen Ali³

¹Department of Computer Science, College of Education for Pure Science/Ibn Al-Haitham, University of Baghdad, Baghdad, Iraq

²Information Technology Unit, College of Education for Human Science-Ibn-Rushed, University of Baghdad, Baghdad, Iraq

³Department of Computer Science, University of Technology, Baghdad, Iraq

ARTICLE INFO

Article history:

Received 28 January 2024

Received in revised form

27 May 2024

Accepted 28 May 2024

Keywords:

Iris recognition

Biometric security

Artificial intelligence

Feature selection

Impersonation prevention

ABSTRACT

Due to advancements in computer science and technology, impersonation has become more common. Today, biometrics technology is widely used in various aspects of people's lives. Iris recognition, known for its high accuracy and speed, is a significant and challenging field of study. As a result, iris recognition technology and biometric systems are utilized for security in numerous applications, including human-computer interaction and surveillance systems. It is crucial to develop advanced models to combat impersonation crimes. This study proposes sophisticated artificial intelligence models with high accuracy and speed to eliminate these crimes. The models use linear discriminant analysis (LDA) for feature extraction and mutual information (MI), along with analysis of variance (ANOVA) for feature selection. Two iris classification systems were developed: one using LDA as an input for the OneR machine learning algorithm and another innovative hybrid model based on a One Dimensional Convolutional Neural Network (HM-1DCNN). The MMU database was employed, achieving a performance measure of 94.387% accuracy for the OneR model. Additionally, the HM-1DCNN model achieved 99.9% accuracy by integrating LDA with MI and ANOVA. Comparisons with previous studies show that the HM-1DCNN model performs exceptionally well, with at least 1.69% higher accuracy and lower processing time.

© 2024 The Authors. Published by IASE. This is an open access article under the CC BY-NC-ND license (<http://creativecommons.org/licenses/by-nc-nd/4.0/>).

1. Introduction

The fields of image classification and biometrics have garnered considerable attention from researchers due to their wide variety of applications in classification and security. Distinguishing physical attributes possessed by individuals can be effectively utilized in recognition systems, including item classification, facial recognition, and personal identification verification (Lateef and Abbas, 2022; Kumar et al., 2019). Computer vision-based biometrics, including iris scanning, fingerprints, and facial recognition, are employed in the creation of effective authentication systems (Al-Dabbas et al., 2023a; Anowar et al., 2021). The utilization of iris identification is a significant method for providing individuals with distinct authentication through the

analysis of their iris architecture. Extensive empirical evidence has demonstrated that this particular biometric authentication method exhibits a high degree of accuracy and reliability (Yang et al., 2019; Shaheed et al., 2021). Iris recognition is often regarded as the most efficacious and reliable method for checking the authenticity of individuals. The rationale behind this phenomenon is that the iris of each individual exhibits unique characteristics, even among siblings or twins, and remains consistent throughout one's lifetime without undergoing any changes associated with the aging process. Consequently, this method of identification is considered to be more secure and less vulnerable to spoofing attacks (Morad and Al-Dabbas, 2020; Al-Waisy et al., 2018). The implementation of iris detection is widely observed in various security contexts, such as the banking industry, access control for limited areas, and numerous modern applications (Azeez, 2021; Taha et al., 2021). Given the diverse range of applications and potential benefits associated with this technology, numerous prominent enterprises, particularly those operating within the security sector, are eagerly anticipating the forthcoming advancements in iris-related

* Corresponding Author.

Email Address: hind.moutaz@ihcoedu.uobaghdad.edu.iq (H. M. Al-Dabbas)

<https://doi.org/10.21833/ijaas.2024.06.010>

Corresponding author's ORCID profile:

<https://orcid.org/0000-0002-3912-2051>

2313-626X/© 2024 The Authors. Published by IASE.

This is an open access article under the CC BY-NC-ND license

(<http://creativecommons.org/licenses/by-nc-nd/4.0/>)

developments (Obaida et al., 2022). Several researchers have successfully deployed iris recognition systems on the Multimedia University (MMU) database, utilizing various classifiers such as machine learning methods like Support Vector Machines (SVM), Convolutional Neural Networks (CNNs), and deep learning models (Alwawi and Althabhwawee, 2022; Karthik and Ramkumar, 2022). Different features were used, like Gabor Wavelet's (GWF), LWF, and Fourier Series (Danlami et al., 2020; Jan et al., 2020). As a result, the deep learning technique is widely used among computer scientists and is therefore considered in this research. This study proposes two iris recognition techniques based on OneR machine learning and the Hybrid Model One Dimensional Convolutional Neural Network (HM-1DCNN). The innovative aspect of this work involves using linear discriminant analysis (LDA) for feature extraction combined with two feature selection methods: MI and Analysis of Variance (ANOVA). The objectives of this research are to develop advanced Artificial Intelligence models with high accuracy and speed to prevent impersonation crimes.

2. Related works

The following works are related studies in iris biometrics for image recognition using various methods.

Danlami et al. (2020) proposed an iris identification system with four stages: feature extraction, matching, preprocessing, and iris image acquisition. They used Legendre wavelet filters and Gabor filters on three different datasets: MMU, UBIRIS, and CASIA. The results from the UBIRIS database showed a significant improvement in recognition accuracy using the Legendre wavelet filter compared to the Gabor filter, with a difference of up to 5.4%. The UBIRIS database achieved excellent and highly accurate results, with an accuracy of 93.80%.

Jan et al. (2020) proposed an iris localization method that preprocesses the input eye image using an order statistic filter and bilinear interpolation. They extract an adaptive threshold from the image's histogram, process the binary image with morphological operators, and determine the pupil's center and radius using centroid and geometry concepts. The iris's outer boundary is marked with the Circular Hough Transform (CHT) and refined using the Fourier series. The method showed high accuracy on three iris datasets: 98.21% for MMU, 98.60% for IITD, and 98.60% for CASIA-Iris.

Szymkowski et al. (2021) proposed a discrete Fast Fourier transform (DFFT) method for the iris-based identity human detection utilizing Principal Component Analysis (PCA). Three methods were used for categorization: artificial neural networks, SVM, and k-nearest neighbors. The databases CASIA-IrisV4 and MMU were used to evaluate the algorithm's accuracy. During the experiments, they looked at a range of splits, such as 50:50 (50% testing set and 50% training set, respectively), as well as 25:75, 75:25, and even 90:10. The SVM algorithm produced the most accurate findings with 86.6%.

Karthik and Ramkumar (2022) proposed a method for segmenting the human iris and tested two different machine learning techniques on an image dataset from an uncontrolled setting. They used CNN and SVM models for iris segmentation. This technique was developed using the MMU iris database. The CNN achieved an average iris segmentation accuracy of 93.9% on test images, while the SVM achieved an average accuracy of 71.6%.

Alwawi and Althabhwawee (2022) proposed an end-to-end human iris recognition system. Employed contrast-limited adaptive histogram equalization (CLAHE) and histogram equalization (HE) techniques after preprocessing and augmenting the MMU dataset. A new 2D CNN based on deep learning technology was employed to categorize iris patterns and extract information. The GPU-based experimental findings demonstrated a high training accuracy of 95.33% while requiring 17:59 minutes to complete 400 epochs.

3. Methodology

This research uses the iris database from Multimedia University (MMU) (Al-Dabbas et al., 2023b). Samples from the MMU iris database are shown in Fig. 1. The MMU database includes images of the irises from both the left and right eyes of 46 individuals, totaling 460 images. The MMU dataset is suitable for this research because it provides a variety of data, with each person having five images of their left eye and five images of their right eye. The chosen database is divided into two parts: 70% for the training set and 30% for the testing set. Each image in the database has undergone several preparation steps. Feature extraction combined with feature selection is applied. Finally, the output classification is generated by HM-1DCNN, as shown in Fig. 2.

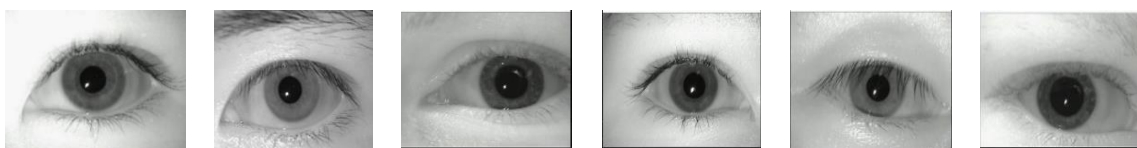


Fig. 1: MMU iris database samples

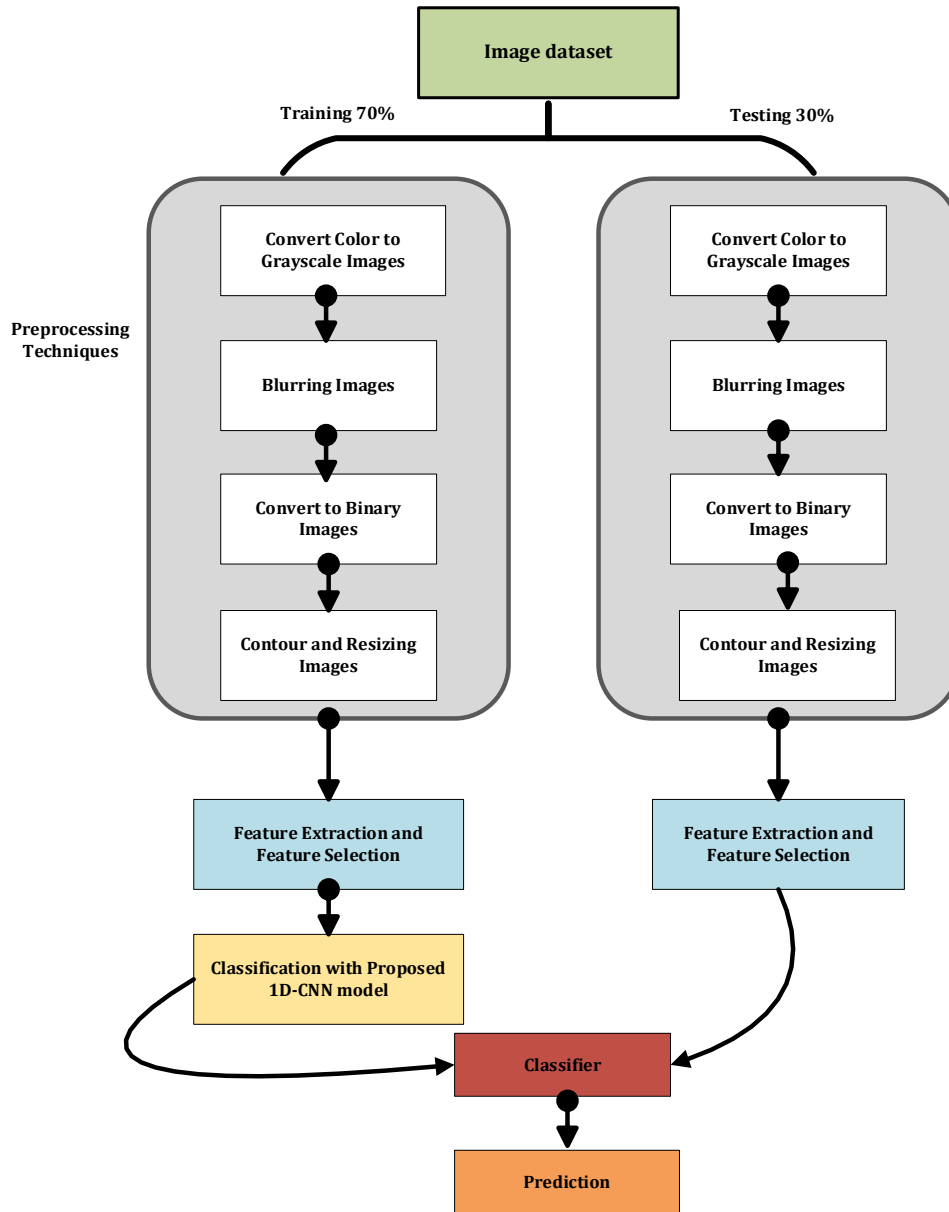


Fig. 2: The system methodology process

3.1. Converting color to grayscale images

The luminance of a grayscale image is often encoded with an eight-bit value. The color of each pixel in a color image is typically represented using a 24-bit value. A primary reason for using grayscale images to extract descriptors, rather than directly using color images, is to simplify the algorithms and reduce computing demands (Mohammed and Al-Dabbas, 2018a; Hadi et al., 2022). To convert a color image to a grayscale image, refer to Eq. 1.

$$greyscale = (0.3 * R) + (0.5 * G) + (0.11 * B) \quad (1)$$

3.2. Blurring images

The phenomenon of blurring involves the perception of enhanced sharpness and detail in an image, enabling the accurate discernment of objects. Blurring is a technique employed to diminish the presence of edge content, resulting in a seamless

transition between colors. For example, the clarity of a facial image is determined by the visibility of the eyes, ears, nose, lips, and forehead (Al-Dabbas et al., 2023b). There exist multiple techniques for attaining the effect of blurring. The median blur filter is commonly employed in this study. The median value of the pixels within the kernel area is utilized as the central component of the image. This operation performs edge processing while simultaneously eliminating noise. The application of the Median Blur filter results in the expansion of color patches inside the image (Al-Dabbas et al., 2023c).

3.3. Converting images to binary format

Binary images have only two possible values: white (1) and black (0). They are also known as 1-bit images because they use only one bit to represent these two values (Obaida et al., 2022). Thresholding is used to convert a grayscale image to a binary image. A threshold value is selected, and gray levels

below this value are set to zero, while gray levels equal to or above the threshold are set to one, as shown in Eq. 2.

$$j(x, y) = \begin{cases} 1 & \text{if } f(x, y) \geq T \\ 0 & \text{otherwise} \end{cases} \quad (2)$$

where, $j(x, y)$ denotes the threshold of the pixel image located in (x, y) while $f(x, y)$ indicates the grayscale pixel image at the same coordinates.

3.4. Contour and resizing images

Contouring image is a computational method employed to identify and extract the structural boundaries of an item seen in an image, subsequently utilizing this information to determine its overall shape and form. The edges are commonly described as having step edges, and their presence is determined by placing markers at specific scales that coincide with the output maxima produced by symmetric and odd filters (Mohammed and Al-Dabbas, 2018b). The input data format was generated by the utilization of bicubic interpolation to resize the photos. The chosen strategy is based on its ability to produce more precise boundaries for the resulting output. In the process of bicubic interpolation, consider the sixteen closest neighboring pixels of a given pixel. Eq. 3 is utilized to determine the value's intensity assigned to the point (x, y) (Abdullah et al., 2016).

$$r(x, y) = \sum_{i=0}^3 \sum_{j=0}^3 a_{ij} x^i y^j \quad (3)$$

where, $r(x, y)$ denotes the function value at the point (x, y) , the coefficients a_{ij} indicates the function values at the 16 data points within the 4x4 grid.

3.5. Feature extraction and feature selection

To reduce the complexity and time required for the proposed system model, ANOVA's discriminative power and MI's comprehensive relationship assessment are combined with LDA feature extraction. This approach aims to identify the most relevant features that significantly impact the target variable. By integrating these methods, we can overcome the limitations of each technique individually while improving model performance, interpretability, and generalizability. This integration offers valuable insights for data analysis practitioners (Benradi et al., 2023).

3.5.1. LDA feature extraction

LDA was employed for the purposes of data visualization, dimensionality reduction, and classification. LDA often yields satisfactory outcomes in terms of classification accuracy, robustness, and interpretability. In the context of addressing real-world classification problems. This method was commonly employed as an inventive. Here are the further LDA steps (Rashed and Hamd, 2021).

Take samples for first class and second class.

- Compute the means of classes denotes as M1 and M2.
- Compute covariance matrices for classes symbolized (C1 and C2)
- Compute the within-class scatter matrix as Eq. 4

$$S_w = C1 + C2 \quad (4)$$

- Create the among-class scatter matrix as Eq. 5 based on the means of the classes determined in step 2.

$$S_B = (M1 - M2) * (M1 - M2) \quad (5)$$

- Compute the means of all classes.
- The fundamental problem with eigenvalues is subsequently answered by the utilization of the LDA technique. As in Eqs. 6 and 7

$$S_w^{-1} S_B W = \lambda W \quad (6)$$

$$W = \text{eig}(S_w^{-1} S_B) \quad (7)$$

where, W is projection vector.

3.5.2. ANOVA feature selection

ANOVA is a group of statistical models, and associated estimation methods are used to evaluate variances in means (Bertinetto et al., 2020). The value of the f-ratio, which is obtained by dividing the variance across classes by the variance within classes, is computed using the equations of ANOVA. A class separation indicator is provided by the size of the f ratio. Data are preserved as features during retention times that result in an f ratio larger than a predetermined threshold, while the rest of the data are deleted. To calculate the variance between classes as follows in Eq. 8:

$$\sigma_{C1}^2 = \frac{\sum(\bar{x}_i - \bar{x})^2 n_i}{(k-1)} \quad (8)$$

where, (x_i) represents the mean value of the i th class, \bar{x} denotes the overall mean, and n_i is the number of measurements in the i th class. To compute the within-class variance in Eq. 9:

$$\sigma_{err}^2 = \frac{\sum \sum (x_{ij} - \bar{x})^2 - (\sum(\bar{x}_i - \bar{x})^2 n_i)}{(N-k)} \quad (9)$$

where, x_{ij} is the j th class's i th measurement. The ratio of the two variances in Eq. 10 is then used to generate an ANOVA f ratio:

$$f \text{ ratio} = \frac{\sigma_{C1}^2}{\sigma_{err}^2} \quad (10)$$

3.5.3. MI feature selection

MI refers to a quantification of the extent to which one random variable possesses knowledge about another. This can be employed to quantify the

degree of relevance between a subset of features and the output vector C, hence proving advantageous within the domain of feature selection. Eq. 11 provides the official description of MI (Seetharaman and Ragupathy, 2012; Saraf et al., 2022):

$$MI(x, y) = \sum_{i=1}^n \sum_{j=1}^n p(x(i), y(j)) \cdot \log \left(\frac{p(x(i), y(j))}{p(x(i)) \cdot p(y(j))} \right) \quad (11)$$

where, MI is zero when x and y are statically independent, i.e., $p(x(i), y(j)) = p(x(i)) \cdot p(y(j))$. Considering two random variables x and y, their joint probability density function is $p(x(i), y(j))$.

3.6. Classification model with one rule (OneR)

The OneR is a classification technique that is characterized by its simplicity and precision. It operates by formulating a rule for each predictor variable in the dataset and thereafter picking the rule that yields the smallest overall error. This algorithm exclusively permits the use of level-one decision trees (Lee and Park, 2022). The One Rule algorithm has one parameter, denoting the threshold for the minimal frequency of an attribute value. In the event that an attribute value is found to have a frequency lower than a predetermined threshold, it is then consolidated with the most commonly occurring value for that particular property. This strategy aids in mitigating the influence of infrequent values on the decision-making process (Singh et al., 2017). The OneR steps are shown in Algorithm 1.

Algorithm 1: Steps of OneR

Input: Extracted Features

Output: Construct classifier

Begin

Step 1: For every predictor,

Step 2: The rule should be generated for every value of the respective predictor.

Step 2.1: Determine the frequency of occurrence for each value inside the target class.

Step 2.2: Identify the class that occurs most frequently.

Step 2.3: The rule assigns a prediction value to the class.

Step 2.4: Calculate the aggregate error for each rule of every predictor.

Step 3: Select the predictor that has the lowest total error.

End

3.7. Architecture of the proposed classification system

CNNs are used for identification and classification. CNNs consist of filters, kernels, or neurons that can learn their parameters, biases, and weights (Suganthi et al., 2022). Each filter receives inputs, performs convolution, and optionally adds nonlinearity. The structure of CNNs includes convolutional, pooling, rectified linear unit (ReLU), and fully connected layers (Wang et al., 2017).

The proposed HM-1DCNN has 26 layers, including eight 1D convolutional layers for feature extraction, six 1D Max-pooling layers, seven

LeakyReLU layers to speed up training by reducing the slope for negative feature values, four fully connected (Dense) layers, and one flatten layer that transforms the output into a single vector for the next stage, as shown in Algorithm 2. This hybrid model outperforms classic deep learning models in prediction performance.

The CNN architecture is detailed in Algorithm 2, with each layer's filters, kernel size, strides (steps), and padding. The dataset is split into 70% for training and 30% for testing. The model runs for 100 epochs with a batch size of 512, using the ADAM optimizer with a learning rate of 0.001. This architecture is suitable for many deep learning applications, including computer vision and natural language processing, and is an enhanced form of stochastic gradient descent. Fig 3 shows the detailed layers of the proposed HM-1DCNN architecture.

Algorithm 2: The Architecture of the proposed HM-1DCNN

Input: features of dataset

Output: CNN with optimum weights

Begin

Step 1: Add Conv1D with (filters=16, input_shape=(43,1), kernel_size=3, strides=1, padding='valid')

Step 2: Add LeakyReLU with (alpha=0.3)

Step 3: Add MaxPooling1D with (pool_size=2, strides=2, padding='valid')

Step 4: Add LeakyReLU with (alpha=0.3)

Step 5: Add Conv1D with (filters=32, kernel_size=3, strides=1, padding='valid')

Step 6: Add MaxPooling1D with (pool_size=2, strides=2, padding='valid')

Step 7: Add Conv1D with (filters=64, kernel_size=3, strides=1, padding='valid')

Step 8: Add LeakyReLU with (alpha=0.3)

Step 9: Add MaxPooling1D with (pool_size=2, strides=2, padding='valid')

Step 10: Add Conv1D with (filters=128, kernel_size=3, strides=1, padding='valid')

Step 11: Add LeakyReLU with (alpha=0.3)

Step 12: Add MaxPooling1D with (pool_size=2, strides=2, padding='valid')

Step 13: Add Conv1D with (filters=256, kernel_size=3, strides=1, padding='same')

Step 14: Add LeakyReLU with (alpha=0.3)

Step 15: Add MaxPooling1D with (pool_size=2, strides=2, padding='valid')

Step 16: Add Conv1D with (filters=512, kernel_size=3, strides=1, padding='same')

Step 17: Add LeakyReLU with (alpha=0.3)

Step 18: Add MaxPooling1D with (pool_size=2, strides=2, padding='valid')

Step 19: Add Conv1D with (filters=1024, kernel_size=3, strides=1, padding='same')

Step 20: Add LeakyReLU with (alpha=0.3)

Step 21: Add Dense with (512, activation='linear')

Step 22: Add Dense with (256, activation='linear')

Step 23: Add Dense with (128, activation='linear')

Step 24: Add Conv1D with (filters=485, kernel_size=1, strides=1, padding='same', activation='linear')

Step 25: Add Flatten ()

Step 26: Add Dense with (44, activation='softmax')

End

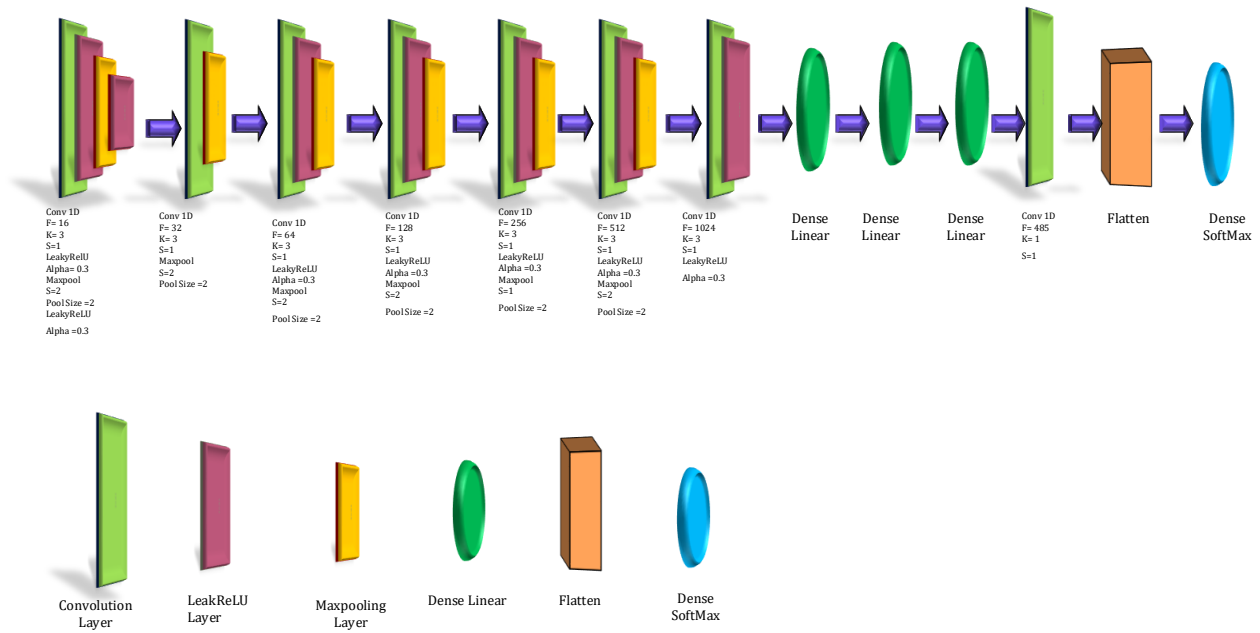


Fig. 3: The proposed HM-1DCNN architecture layers

3.8. Performance measures

The suggested hybrid algorithms' performance is evaluated using various criteria (Chicho et al., 2021; Szymkowski et al., 2021).

- Accuracy: the percentage of instances properly classified out of all those presented. it can be calculated as in Eq. 12.

$$\text{Accuracy} = \frac{\text{TN} + \text{TP}}{\text{TN} + \text{FP} + \text{FN} + \text{TP}} \tag{12}$$

- Precision: represents the correction ratio of predicting the positive results is evaluated as in Eq. 13.

$$\text{Precision} = \frac{\text{TP}}{\text{TP} + \text{FP}} \tag{13}$$

- Recall: represents the ability to identify all pertinent instances within a given dataset, as denoted by Eq. 14.

$$\text{Recall} = \frac{\text{TP}}{\text{TP} + \text{FN}} \tag{14}$$

- F1-measure is the harmonic mean of recall, and precision is calculated as in Eq. 15

$$F_1 = \frac{1}{\frac{1}{\text{recall}} + \frac{1}{\text{precision}}} = 2 * \frac{\text{precision} * \text{recall}}{\text{precision} + \text{recall}} \tag{15}$$

4. Results and discussion

4.1. Time performance

The processing time for this model is considered efficient and low. Using LDA feature extraction alone, the total training time was 900 seconds, with each epoch taking 4 seconds over 100 epochs and a batch size of 512. When LDA feature extraction was

combined with MI and ANOVA feature selection, the training time ranged between 240 and 300 seconds, with each epoch taking 2 seconds over 100 epochs and a batch size of 512. These results are considered very good compared to other researchers' models.

4.2. Statistical merging features performance

LDA applied with OneR machine learning achieved good results, with an accuracy of 94.387%, precision of 94.387%, recall of 94.895%, and an F1-measure of 94.527%. However, applying HM-1DCNN yielded remarkable results, with an accuracy of 99.22% and 99.33% for precision, recall, and F1-measure. When merging 5% and 10% of ANOVA and MI with LDA, the performance was good, with an accuracy of 99% and consistently high precision, recall, and F1-measure between 99% and 99.5%. When merging 15% and 20%, the performance was outstanding, reaching 99.8% and 99.9% for precision, recall, and F1-measure. These results highlight the potential of combining features from ANOVA and MI at different percentages to enhance predictive capabilities and model efficiency, as shown in Table 1. Comparing these proposed systems' outputs with previous related works using the MMU database and various feature extraction and classification methods, such as GWF, LWF, and Fourier Series with classifiers like SVM, CNN, and deep learning models, the accuracy ranged from 93.00% to 98.21%. In contrast, the two proposed systems achieved very high accuracy and quick processing. HM-1DCNN is considered superior to OneR. Table 2 illustrates the comparison.

5. Conclusions

High accuracy and faster performance models are presented in this study. The feature extraction

method, LDA, is used as an input for the OneR machine learning model and a novel HM-1DCNN, which combines LDA with MI and ANOVA feature

selection methods. The MMU database was processed using preprocessing techniques.

Table 1: Results of the proposed model

Classifier	Accuracy	Precision	Recall	F1-score
LDA + OneR ML	94.387%	94.387 %	94.895 %	94.527 %
LDA+ HM-1DCNN	99.22%	99.33%	99.33%	99.33%
LDA+ 5% (ANOVA and MI) + HM-1DCNN	99%	99.5%	99%	99%
LDA+ 10% (ANOVA and MI) + HM-1DCNN	99%	99.4%	99%	99%
LDA+ 15% (ANOVA and MI) + HM-1DCNN	99.8%	99.8%	99%	99%
LDA+ 20% (ANOVA and MI) + HM-1DCNN	99.9%	99.9%	99.9%	99.9%

Table 2: Comparative analysis of the proposed system and related works

Methods of previous works	Feature extraction	Classifier	Accuracy
(Karthik and Ramkumar, 2022)	-	SVM	72.00%
		CNN	94.00%
(Danlami et al., 2020)	GWF, LWF	-	93.00%
		k-nearest neighbors	93.80%
(Szymkowski et al., 2021)		SVM	92.10%
		Artificial neural network	98.4%
(Alwawi and Althabhaawee, 2022)	-	deep learning	94.1%
(Jan et al., 2020)	Fourier Series	-	95.33%
Proposed work	LDA	OneR	98.21
Proposed work	LDA with ANOVA and MI	HM-1DCNN	94.387 %
			99.9%

Several measures were used to evaluate the performance of the proposed classification systems, including accuracy, precision, recall, and the F1-measure. The LDA feature extraction with OneR ML achieved an accuracy of 94.387%, precision of 94.387%, recall of 94.895%, and an F1-measure of 94.527%. In contrast, LDA with HM-1DCNN achieved 99.22% accuracy and 99.33% for precision, recall, and F1-measure.

When combining LDA with different percentages of MI and ANOVA feature selection (5%, 10%, 15%, and 20%), the best performance was achieved with 99.9% for accuracy, precision, recall, and F1-measure. The processing time was also efficient, taking 4 seconds per epoch out of 100 epochs with a batch size of 512. When merging LDA with MI and ANOVA, the time reduced to 2 seconds per epoch.

These findings are excellent compared to other models. Integrating AI techniques aims to create a highly secure system in terms of accuracy and speed, making it applicable in real-world scenarios. Machine learning and deep learning classifiers are used in various industries to improve recognition performance, predict customer behavior, classify medical conditions, and analyze large datasets for better business decisions in fields like finance and healthcare.

Compliance with ethical standards

Conflict of interest

The author(s) declared no potential conflicts of interest with respect to the research, authorship, and/or publication of this article.

References

Abdullah MA, Dlay SS, Woo WL, and Chambers JA (2016). Robust iris segmentation method based on a new active contour force

with a noncircular normalization. *IEEE Transactions on Systems, Man, and Cybernetics: Systems*, 47(12): 3128-3141. <https://doi.org/10.1109/TSMC.2016.2562500>

Al-Dabbas HM, Azeez RA, and Ali AE (2023a). Digital watermarking, methodology, techniques, and attacks: A review. *Iraqi Journal of Science*, 41: 4169-4186. <https://doi.org/10.24996/ijcs.2023.64.8.37>

Al-Dabbas HM, Azeez RA, and Ali AE (2023b). Machine learning approach for facial image detection system. *Iraqi Journal of Science*, 64(10): 5428-5441. <https://doi.org/10.24996/ijcs.2023.64.10.44>

Al-Dabbas HM, Azeez RA, and Ali AE (2023c). Efficient iris image recognition system based on machine learning approach. *Iraqi Journal of Computers, Communications, Control and Systems Engineering*, 23(3): 104-114. <https://doi.org/10.33103/uot.ijccce.23.3.9>

Al-Waisy AS, Qahwaji R, Ipson S, Al-Fahdawi S, and Nagem TA (2018). A multi-biometric iris recognition system based on a deep learning approach. *Pattern Analysis and Applications*, 21: 783-802. <https://doi.org/10.1007/s10044-017-0656-1>

Alwawi BKO C and Althabhaawee AFY (2022). Towards more accurate and efficient human iris recognition model using deep learning technology. *Telecommunication Computing Electronics and Control*, 20(4): 817-824. <https://doi.org/10.12928/telkomnika.v20i4.23759>

Anowar F, Sadaoui S, and Selim B (2021). Conceptual and empirical comparison of dimensionality reduction algorithms (PCA, KPCA, LDA, MDS, SVD, LLE, ISOMAP, LE, ICA, t-SNE). *Computer Science Review*, 40: 100378. <https://doi.org/10.1016/j.cosrev.2021.100378>

Azeez RA (2021). Determination efficient classification algorithm for credit card owners: Comparative study. *Engineering and Technology Journal*, 39(1B): 21-29. <https://doi.org/10.30684/etj.v39i1B.1577>

Benradi H, Chater A, and Lasfar A (2023). A hybrid approach for face recognition using a convolutional neural network combined with feature extraction techniques. *IAES International Journal of Artificial Intelligence*, 12(2): 627-640. <https://doi.org/10.11591/ijai.v12.i2.pp627-640>

Bertinetto C, Engel J, and Jansen J (2020). ANOVA simultaneous component analysis: A tutorial review. *Analytica Chimica Acta*, X, 6: 100061. <https://doi.org/10.1016/j.acax.2020.100061>
PMid:33392497 PMCID:PMC7772684

- Chicho BT, Abdulazeez AM, Zeebaree DQ, and Zebari DA (2021). Machine learning classifiers based classification for iris recognition. *Qubahan Academic Journal*, 1(2): 106-118. <https://doi.org/10.48161/qaj.v1n2a48>
- Danlami M, Jamel S, Ramli SN, and Azahari SRM (2020). Comparing the legendre wavelet filter and the Gabor wavelet filter for feature extraction based on iris recognition system. In the 6th International Conference on Optimization and Applications (ICOA), IEEE, Beni Mellal, Morocco: 1-6. <https://doi.org/10.1109/ICOA49421.2020.9094465>
- Hadi WJ, Kadhem SM, and Abbas AR (2022). Detecting deepfakes with deep learning and Gabor filters. *ARO: The Scientific Journal of Koya University*, 10(1): 18-22. <https://doi.org/10.14500/aro.10917>
- Jan F, Min-Allah N, Agha S, Usman I, and Khan I (2020). A robust iris localization scheme for the iris recognition. *Multimedia Tools and Applications*, 80: 4579-4605. <https://doi.org/10.1007/s11042-020-09814-5>
- Karthik B and Ramkumar G (2022). Comparison of feature extraction technique for segmentation in human iris recognition under uncontrolled environment using CNN algorithm with SVM classifier. *ECS Transactions*, 107(1): 16785-16795. <https://doi.org/10.1149/10701.16785ecst>
- Kumar A, Kaur A, and Kumar M (2019). Face detection techniques: A review. *Artificial Intelligence Review*, 52: 927-948. <https://doi.org/10.1007/s10462-018-9650-2>
- Lateef RA and Abbas AR (2022). Tuning the hyperparameters of the 1D CNN model to improve the performance of human activity recognition. *Engineering and Technology Journal*, 40(04): 547-554. <https://doi.org/10.30684/etj.v40i4.2054>
- Lee YW and Park KR (2022). Recent iris and ocular recognition methods in high-and low-resolution images: A survey. *Mathematics*, 10(12): 2063. <https://doi.org/10.3390/math10122063>
- Mohammed FG and Al-Dabbas HM (2018a). The effect of wavelet coefficient reduction on image compression using DWT and Daubechies wavelet transform. *Science International*, 30(5): 757-762.
- Mohammed FG and Al-Dabbas HM (2018b). Application of WDR technique with different wavelet codecs for image compression. *Iraqi Journal of Science*, 59(4): 2128-2134. <https://doi.org/10.24996/ijs.2018.59.4B.18>
- Morad AH and Al-Dabbas HM (2020). Classification of brain tumor area for MRI images. In the 1st International Conference on Pure Science (ISCPS). *Journal of Physics: Conference Series*, 1660(1): 012059. <https://doi.org/10.1088/1742-6596/1660/1/012059>
- Obaida TH, Hassan NF, and Jamil AS (2022). Comparative of Viola-Jones and YOLO v3 for face detection in real time. *Iraqi Journal of Computers, Communications, Control and Systems Engineering* 22: 63-72. <https://doi.org/10.33103/uot.ijccce.22.2.6>
- Rashed AH and Hamd MH (2021). Robust detection and recognition system based on facial extraction and decision tree. *Journal of Engineering and Sustainable Development*, 25(4): 40-50. <https://doi.org/10.31272/jeasd.25.4.4>
- Saraf TOQ, Fuad N and Taujuddin NSAM (2022). Feature encoding and selection for iris recognition based on variable length black hole optimization. *Computers*, 11(9): 140. <https://doi.org/10.3390/computers11090140>
- Seetharaman K and Ragupathy R (2012). Iris recognition for personal identification system. *Procedia Engineering*, 38: 1531-1546. <https://doi.org/10.1016/j.proeng.2012.06.189>
- Shaheed K, Mao A, Qureshi I, Kumar M, Abbas Q, Ullah I, Zhang X (2021). A systematic review on physiological-based biometric recognition systems: Current and future trends. *Archives of Computational Methods in Engineering*, 28: 4917-4960. <https://doi.org/10.1007/s11831-021-09560-3>
- Singh J, Singh G, and Singh R (2017). Optimization of sentiment analysis using machine learning classifiers. *Human-Centric Computing and Information Sciences*, 7(1): 1-12. <https://doi.org/10.1186/s13673-017-0116-3>
- Suganthi ST, Ayoobkhan MUA, Bacanin N, Venkatachalam K, Štěpán H, and Pavel T (2022). Deep learning model for deep fake face recognition and detection. *PeerJ Computer Science*, 8: e881. <https://doi.org/10.7717/peerj-cs.881>
PMid:35494811 PMCID:PMC9044351
- Szymkowski M, Jasiński P, and Saeed K (2021). Iris-based human identity recognition with machine learning methods and discrete fast Fourier transform. *Innovations in Systems and Software Engineering*, 17(3): 309-317. <https://doi.org/10.1007/s11334-021-00392-9>
- Taha NA, Qasim Z, Al-Saffar A, and Abdullatif AA (2021). Steganography using dual tree complex wavelet transform with LSB indicator technique. *Periodicals of Engineering and Natural Sciences*, 9(2): 1106-1114. <https://doi.org/10.21533/pen.v9i2.2060>
- Wang R, Li W, Qin R, and Wu J (2017). Blur image classification based on deep learning. In the International Conference on Imaging Systems and Techniques (IST), IEEE, Beijing, China: 1-6. <https://doi.org/10.1109/IST.2017.8261503>
- Yang W, Wang S, Hu J, Zheng G, and Valli C (2019). Security and accuracy of fingerprint-based biometrics: A review. *Symmetry*, 11(2): 141. <https://doi.org/10.3390/sym11020141>